Photocatalytic Efficacy of Heterocyclic Base Grafted Chitosan Magnetite Nanoparticles on Sorption of Pb(II); Application on Mining Effluent

Mohammed F. Hamza [1,2,*], Adel E.-S. Goda [3], Shunyan Ning [2], Hamed I. Mira [2], Adel A.-H. Abdel-Rahman [4], Yuezhou Wei [1,5,*], Toyohisa Fujita [6,7], Hamada H. Amer [8], Saad H. Alotaibi [8] and Amr Fouda [9]

[1] School of Nuclear Science and Technology, University of South China, Hengyang 421001, China
[2] Nuclear Materials Authority, POB 530, El-Maadi, Cairo 11728, Egypt; ningshunyan@usc.edu.cn (S.N.); hamedmira@yahoo.com (H.I.M.)
[3] Tanta Higher Institute of Engineering and Technology, Tanta 31739, Egypt; adelgoda1969@gmail.com
[4] Chemistry Department, Faculty of Science, Menofia University, Shebin El-Kom 32511, Egypt; adelnassar63@yahoo.com
[5] School of Nuclear Science and Engineering, Shanghai Jiao Tong University, Shanghai 200240, China
[6] School of Resources, Environment and Materials, Guangxi University, Nanning 530004, China; fujitatoyohisa@gxu.edu.cn
[7] School of Chemistry and Chemical Engineering, Guangxi University, Nanning 530004, China
[8] Department of Chemistry, Turabah University College, Taif University, Taif 21944, Saudi Arabia; h.amer@tu.edu.sa (H.H.A.); s.alosaimi@tu.edu.sa (S.H.A.)
[9] Botany and Microbiology Department, Faculty of Science, Al-Azhar University, Cairo 11884, Egypt; amr_fh83@azhar.edu.eg
* Correspondence: m_fouda21@hotmail.com (M.F.H.); yzwei@sjtu.edu.cn (Y.W.); Tel.: +20-111-668-1228 (M.F.H.); +86-771-322-4990 (Y.W.)

Table S1. Diffraction patterns of the XRD peaks and the matched reference file.

Pos. [°2Th.]	d-spacing [Å]	Rel. Int. [%]	Matched by
18.2700	4.85595	17.16	01-077-1545
30.2500	2.95462	17.16	01-077-1545
35.5474	2.52552	100.00	01-077-1545
37.3469	2.40787	17.16	01-077-1545
43.1967	2.09438	35.60	01-077-1545
57.0873	1.61342	33.87	01-077-1545
62.6265	1.48338	47.67	01-077-1545
81.4031	1.18220	17.83	01-077-1545
82.2235	1.17150	14.80	01-077-1545

Table S2. Elemental analysis of MCc and MCa-ATA sorbents.

		C	N	H	O	Fe	S
MCc	%	28.15	4.92	3.99	32.18	30.76	0
	mmol	23.44	3.51	39.58	20.11	5.51	0
MCa-ATA	%	26.44	6.48	4.1	33.03	27.1	2.85
	mmol	22.02	4.63	40.68	20.65	4.853	0.89

Table S3. Chemical composition of the ferruginous sandstone ore material.

Major Oxides	Conc., (%)	Trace Elements	Conc. (ppm)
SiO_2	40.0	U	2600
TiO_2	0.33	Ni	138
Al_2O_3	3.40	Pb	900
Fe_2O_3	26.0	B	200
CaO	1.20	Cu	165
MgO	3.20	V	150
MnO	1.80	Zr	180
Na_2O	0.90	Th	60
K_2O	0.70		
P_2O_5	3.60		
RE_2O_3	12.6		
L.O.I *	4.06		
Total	97.79		

L.O.I *: loss of ignition.

Table S4. Chemical composition of the the ore leachates and the produced effluents after extraction treatments.

Ore leachate		After loading/ pH control and PPT	
Metal ion	**Conc. mg g^{-1}**	**Conc. mg g^{-1}**	**removing %**
Si(IV)	128	92.26	27.921875
Al(III)	8170	98.7	98.7919217
Fe(III)	20800	60.54	99.7089423
Ca(II)	1170	499.3	57.3247863
Mn(II)	980	504.8	48.4897959
Ni(II)	60.8	36.59	39.8190789
Cu(II)	31.5	10.1	67.9365079
REE(III)	8700	48.95	99.4373563
U(VI)	200	18.1	90.95
Pb(II)	80.31	38.97	51.4755323

Table S5a. Reminder on equations used for modeling uptake kinetics **[94–96]**.

Model	Equation	Parameters	Ref.
PFORE	$$q(t) = q_{eq,1}(1 - e^{-k_1 t})$$	$q_{eq,1}$ (mmol g^{-1}): sorption capacity at equilibrium k_1 (min^{-1}): apparent rate constant of PFORE	[96]
PSORE	$$q(t) = \frac{q_{eq,2}^2 k_2 t}{1 + k_2 q_{eq,2} t}$$	$q_{eq,2}$ (mmol g^{-1}): sorption capacity at equilibrium k_2 (g mmol^{-1} min^{-1}): apparent rate constant of PSORE	[96]
RIDE	$$\frac{q(t)}{q_{eq}} = 1 - \sum_{n=1}^{\infty} \frac{6\alpha(\alpha + 1)\exp\left(\frac{-D_e q_n^2}{r^2}t\right)}{9 + 9\alpha + q_n^2\alpha^2}$$ With q_n being the non-zero roots of $\tan q_n = \frac{3\,q_n}{3 + \alpha q_n^2}$ and $\quad \frac{m\,q}{V\,C_0} = \frac{1}{1+\alpha}$	D_e (m^2 min^{-1}) : Effective diffusivity coefficient	[94]

(m (g): mass of sorbent; V (L): volume of solution; C_0 (mmol L^{-1}): initial concentration of the solution).

Table S5b. Reminder on equations used for modeling sorption isotherms [95,97,98].

Model	Equation	Parameters	Ref.
Langmuir	$$q_{eq} = \frac{q_{m,L}C_{eq}}{1 + b_L C_{eq}}$$	$q_{m,L}$ (mmol g^{-1}): Sorption capacity at saturation of monolayer b_L (L mmol^{-1}): Affinity coefficient	[95]
Freundlich	$$q_{eq} = k_F C_{eq}^{1/n_F}$$	k_F and n_F: empirical parameters of Freundlich equation	[95]
Sips	$$q_{eq} = \frac{q_{m,s}b_S C_{eq}^{1/n_S}}{1 + b_S C_{eq}^{1/n_S}}$$	$q_{m,L}$, b_S and n_S: empirical parameters of Sips equation (based on Langmuir and Freundlich equations)	[95]
Temkin	$$q_{eq} = \frac{R\,T}{b_T}\ln(A_T C_{eq})$$	b_T: J kg mol^{-2}, Temkin isotherm constant A_T: L mol^{-1}, Temkin isotherm equilibrium constant	[98]

Akaike Information Criterion, AIC [99]:

$$AIC = N \ln\left(\frac{\sum_{i=0}^{N}(y_{i,exp.} - y_{i,model})^2}{N}\right) + 2N_p + \frac{2N_p(N_p + 1)}{N - N_p - 1}$$

where N is the number of experimental points, N_P the number of model parameters, $y_{i,exp.}$ and $y_{i,model}$ the experimental and calculated values of the tested variable.
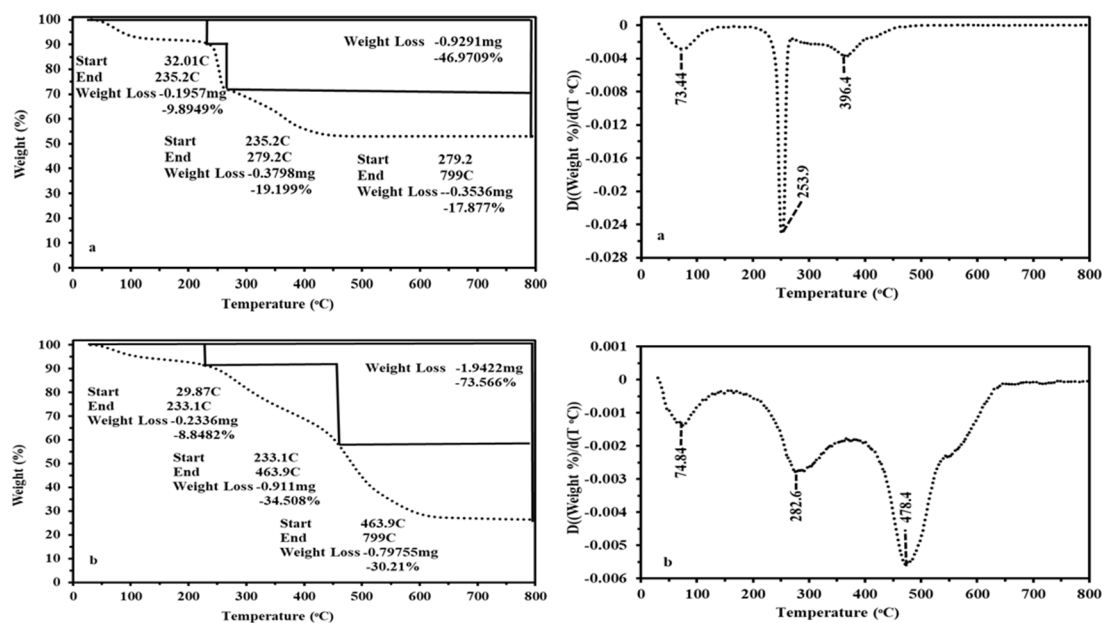
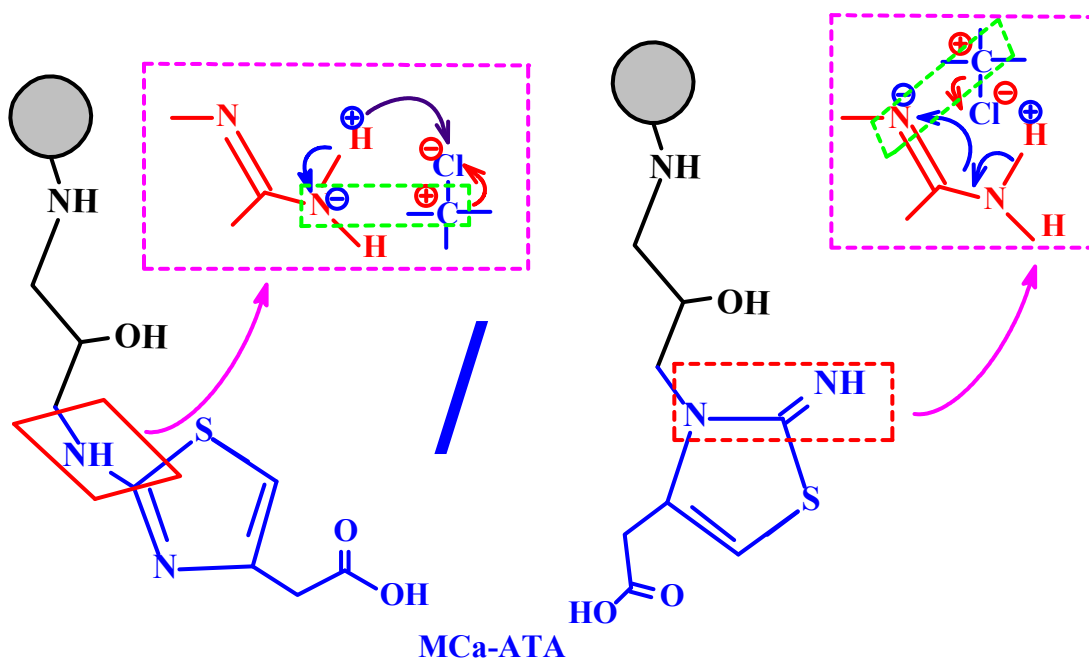**Figure S1.** TGA and Dr-TGA of MCc (**a**) and MCa-ATA (**b**).

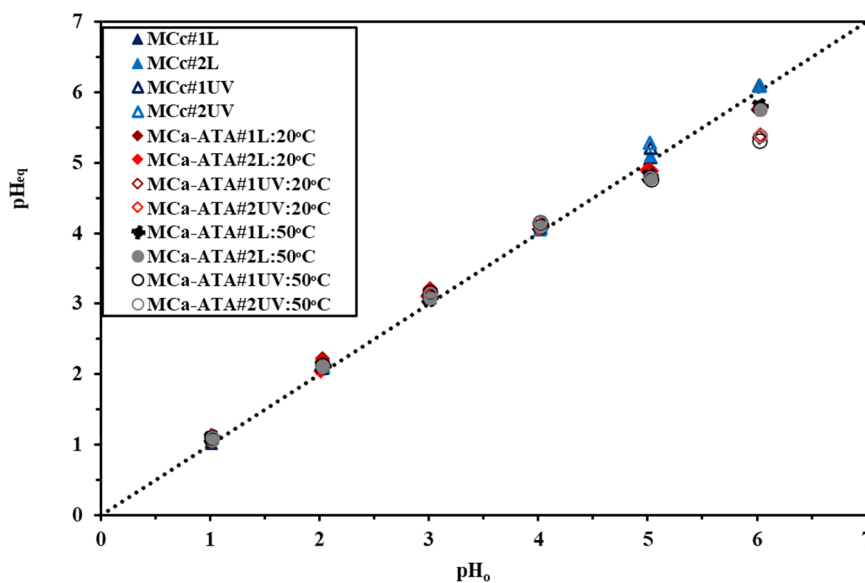**Figure S2.** Tautomerization of the functionalized sorbent at a mild pH conditions.

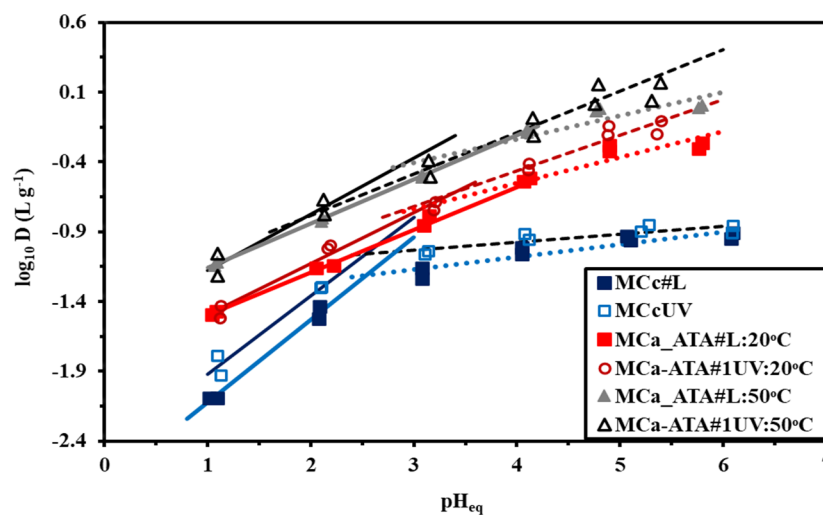**Figure S3.** pH variation of MCc and MCa-ATA at 20 and 50 °C under light and UV effect.

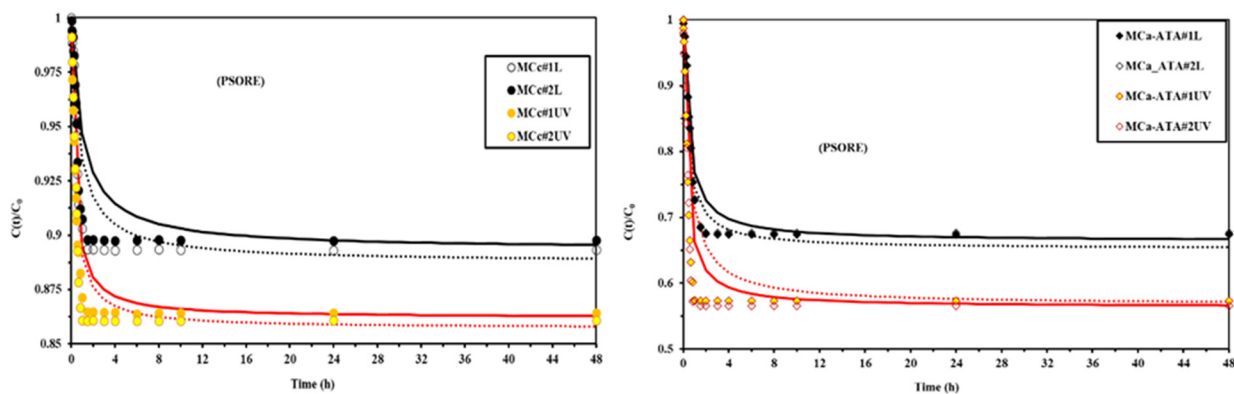**Figure S4.** The data collected from plotting of the $\log_{10}D$ and the equilibrium pH.

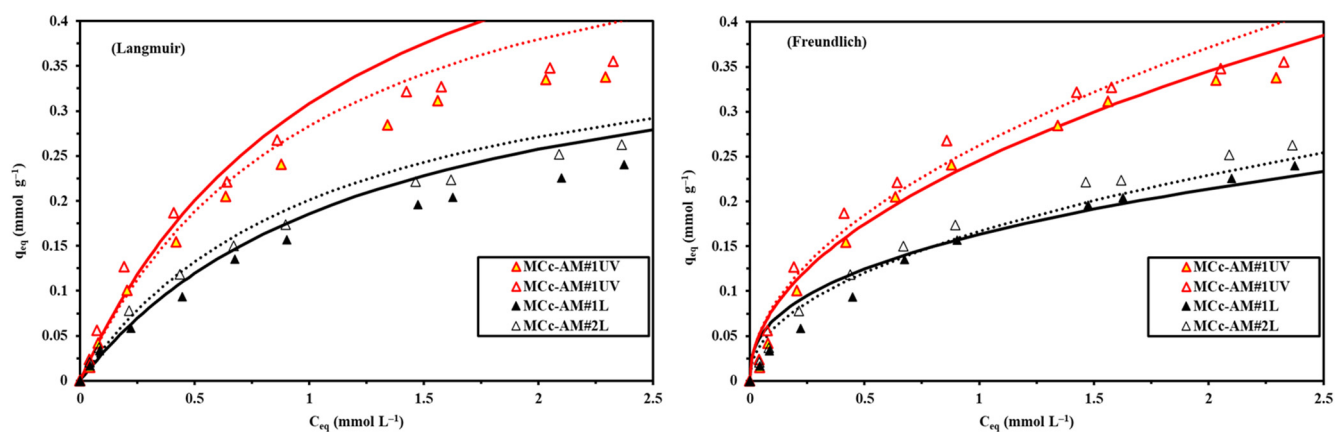**Figure S5.** Sorption kinetics of MCc and MCa-ATA for the PSORE at light and UV effect.

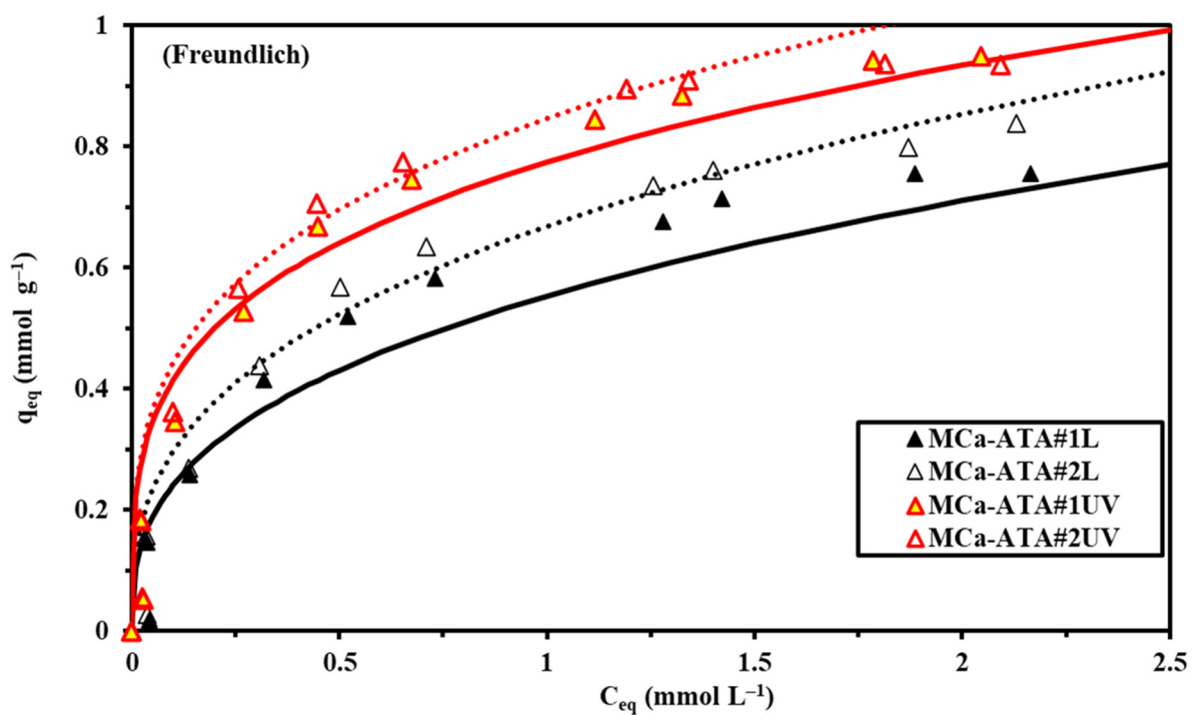**Figure S6.** Sorption Isotherms (Langmuir and Freundlich) models of the MCc sorbent at light and

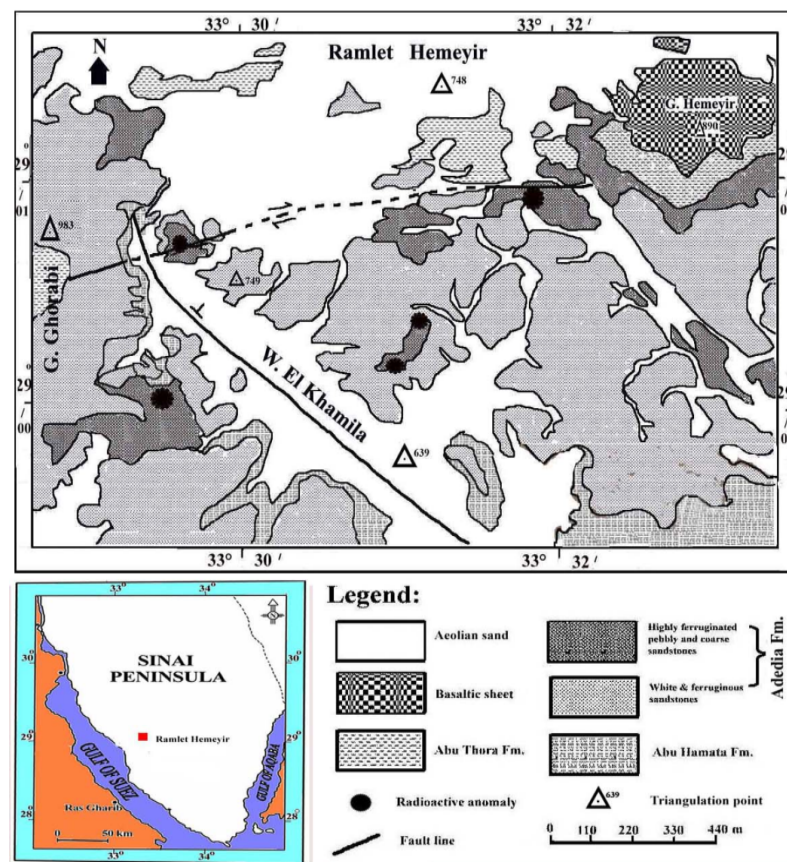**Figure S7.** Sorption Isotherms (Freundlich) model of the MCa-ATA sorbent at light and UV.

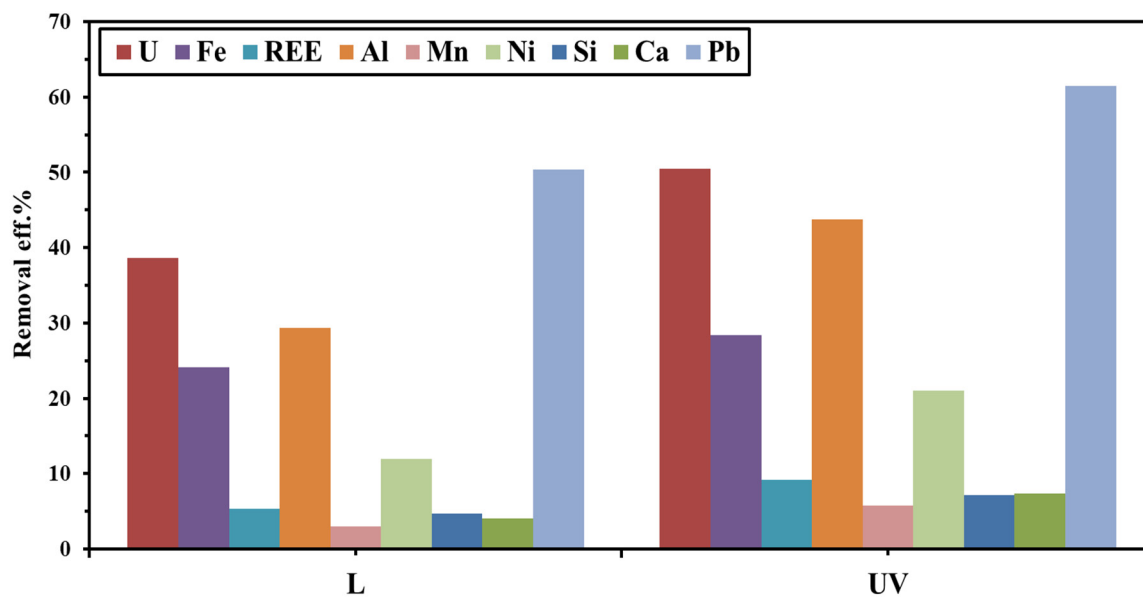**Figure S8.** Geological map of the studied area.

Figure S9. Removal efficiency % of metal ions in the ore effluent after treatment with MCa-ATA under light and UV conditions.